



A Full Eulerian Wave-Body Interaction Solver for Incompressible Two-Phase Flows with High Density and Viscosity Ratios

Farahbakhsh, Iman ; Amini-Afshar, Mostafa; Bingham, Harry B.

Publication date:
2023

Document Version
Peer reviewed version

[Link back to DTU Orbit](#)

Citation (APA):

Farahbakhsh, I., Amini-Afshar, M., & Bingham, H. B. (2023). *A Full Eulerian Wave-Body Interaction Solver for Incompressible Two-Phase Flows with High Density and Viscosity Ratios*. Paper presented at 38th IWWWFB, Ann Arbor, Michigan, United States.

General rights

Copyright and moral rights for the publications made accessible in the public portal are retained by the authors and/or other copyright owners and it is a condition of accessing publications that users recognise and abide by the legal requirements associated with these rights.

- Users may download and print one copy of any publication from the public portal for the purpose of private study or research.
- You may not further distribute the material or use it for any profit-making activity or commercial gain
- You may freely distribute the URL identifying the publication in the public portal

If you believe that this document breaches copyright please contact us providing details, and we will remove access to the work immediately and investigate your claim.

A Full Eulerian Wave-Body Interaction Solver for Incompressible Two-Phase Flows with High Density and Viscosity Ratios

Iman Farahbakhsh¹, Mostafa Amini-Afshar² and Harry B. Bingham²

¹Department of Maritime Engineering, Amirkabir University of Technology, Tehran, Iran
i.farahbakhsh@aut.ac.ir

²Department of Civil & Mechanical Engineering, Technical University of Denmark
maaf@dtu.dk, hbhi@dtu.dk

1 Introduction

A force-free immersed boundary method is developed based on a primitive variable formulation of the Navier-Stokes equations, using Chorin's projection method. In the proposed method, the predetermined motion of a rigid structure is considered, and the rigid domain velocity field is imposed on the formulation by patching the rigid-body motion onto the fluid domain velocity field in the predictor step of the formulation. The capability of the method in handling two-phase fluid interaction with a structure is examined. For a two-phase fluid with large density and viscosity ratios, the Laplacian operator becomes discontinuous. The interface evolution under the effect of an oscillating heaving cylinder based on the setup presented in [1] is considered. Before examining the method's accuracy in solving fluid-structure interaction (FSI) problems comprising two fluids with high density and viscosity ratio, the classical problem of an oscillating cylinder in a quiescent fluid is considered, and the results are compared with [2] and [3].

2 Governing Equations

Using Chorin's projection method based on the Helmholtz-Hodge theorem, the primitive formulation of the Navier-Stokes equation can be expressed in the following form

$$\frac{\mathbf{V}^* - \mathbf{V}^n}{\delta t} = -(\mathbf{V}^n \cdot \nabla)\mathbf{V}^n + \nu \nabla^2 \mathbf{V}^n, \quad (1)$$

$$\mathbf{V}^{n+1} = \mathbf{V}^* - \frac{\delta t}{\rho} \nabla \mathcal{P}^{n+1}, \quad (2)$$

$$\nabla \cdot \mathbf{V}^{n+1} = 0, \quad (3)$$

$$\nabla^2 \mathcal{P}^{n+1} = \frac{\rho}{\delta t} \nabla \cdot \mathbf{V}^*, \quad (4)$$

where $\mathbf{V} = [u, v]$ is the fluid velocity vector (in 2D), \mathcal{P} is the dynamic pressure, ρ, ν are the fluid density and kinematic viscosity, δt is the time-step size and superscript $n = 0, 1, \dots$, is the time step number. The foregoing equations can be redefined for two phase flow by considering the one-fluid formulation and a variable definition of the kinematic viscosity and density. For achieving an smooth distribution at the interface, a re-initializing process must be executed during numerical integration in time. The initial distribution and re-initializing process can be

expressed as follows

$$\Gamma = \{\mathbf{x} | \phi(\mathbf{x}, t) = 0.5\} \quad (5)$$

$$\phi(\mathbf{x}, t) = \begin{cases} > 0.5, & \mathbf{x} \in \text{low density fluid} \\ = 0.5, & \mathbf{x} \in \Gamma \\ < 0.5, & \mathbf{x} \in \text{high density fluid} \end{cases} \quad (6)$$

$$\phi(\mathbf{x}, t) = \begin{cases} 0, & \phi(\mathbf{x}, t) < 0.5 \text{ and } |\bar{\mathbf{x}}| > \lambda \\ (1 + e^{\alpha\bar{\mathbf{x}}/\lambda})^{-1}, & \phi(\mathbf{x}, t) < 0.5 \text{ and } |\bar{\mathbf{x}}| \leq \lambda \\ 0.5, & \phi(\mathbf{x}, t) = 0.5 \text{ or } \bar{\mathbf{x}} = 0 \\ (1 + e^{-\alpha\bar{\mathbf{x}}/\lambda})^{-1}, & \phi(\mathbf{x}, t) > 0.5 \text{ and } |\bar{\mathbf{x}}| \leq \lambda \\ 1, & \phi(\mathbf{x}, t) > 0.5 \text{ and } |\bar{\mathbf{x}}| > \lambda, \end{cases} \quad (7)$$

where, $\bar{\mathbf{x}}$ denotes the distance vector in space to the interface, and $\lambda = \alpha\Delta x$ that $\alpha > 1$. To capture the interface evolution the level set transport equation is solved based on an updated velocity field.

$$\frac{\partial\phi}{\partial t} + \mathbf{V} \cdot \nabla\phi = 0. \quad (8)$$

For regularizing the viscosity and the inverse of the density, a discrete convolution is used in practice [4] as follows.

$$16\tilde{\mu}_{i,j} = 4\mu_{i,j} + 2\mu_{i+1,j} + 2\mu_{i-1,j} + 2\mu_{i,j+1} + 2\mu_{i,j-1} \\ + \mu_{i+1,j+1} + \mu_{i+1,j-1} + \mu_{i-1,j+1} + \mu_{i-1,j-1}, \quad (9)$$

$$\frac{16}{\tilde{\rho}_{i,j}} = \frac{4}{\rho_{i,j}} + \frac{2}{\rho_{i+1,j}} + \frac{2}{\rho_{i-1,j}} + \frac{2}{\rho_{i,j+1}} + \frac{2}{\rho_{i,j-1}} \\ + \frac{1}{\rho_{i+1,j+1}} + \frac{1}{\rho_{i+1,j-1}} + \frac{1}{\rho_{i-1,j+1}} + \frac{1}{\rho_{i-1,j-1}}, \quad (10)$$

where i, j are the discrete control volume indices. It should be noted that ν in equation (1) is calculated based on the regularized density and viscosity of equations (9) and (10). In using two phase model one will encounter a discontinuous Laplacian operator in the pseudo pressure Poisson equation. Here the discretized form of this equation is expressed. For imposing the structure velocity field to the fluid velocity field, the predetermined velocity field is patched onto the velocity field in the predictor stage of the solution. This non-solenoidal patching is corrected during the corrector stage and a full Eulerian monolithic solver is formed.

$$\nabla \cdot [\mathbf{V}^{n+1} = \mathbf{V}^* - \frac{\delta t}{\rho} \nabla \mathcal{P}^{n+1}] \quad (11)$$

$$\nabla \cdot \left[\frac{1}{\rho} \nabla \mathcal{P}^{n+1} \right] = \frac{1}{\delta t} \nabla \cdot \mathbf{V}^* \quad (12)$$

$$\left[\frac{1}{\tilde{\rho}_{i,j}\delta x^2} \left(1 + \frac{\tilde{\rho}_{i+1,j} - \tilde{\rho}_{i-1,j}}{4\tilde{\rho}_{i,j}} \right) \right] \mathcal{P}_{i-1,j}^{n+1} + \left[\frac{1}{\tilde{\rho}_{i,j}\delta x^2} \left(1 - \frac{\tilde{\rho}_{i+1,j} - \tilde{\rho}_{i-1,j}}{4\tilde{\rho}_{i,j}} \right) \right] \mathcal{P}_{i+1,j}^{n+1} + \\ \left[\frac{1}{\tilde{\rho}_{i,j}\delta y^2} \left(1 + \frac{\tilde{\rho}_{i,j+1} - \tilde{\rho}_{i,j-1}}{4\tilde{\rho}_{i,j}} \right) \right] \mathcal{P}_{i,j-1}^{n+1} + \left[\frac{1}{\tilde{\rho}_{i,j}\delta y^2} \left(1 - \frac{\tilde{\rho}_{i,j+1} - \tilde{\rho}_{i,j-1}}{4\tilde{\rho}_{i,j}} \right) \right] \mathcal{P}_{i,j+1}^{n+1} - \\ \left[\frac{2}{\tilde{\rho}_{i,j}} \left(\frac{1}{\delta x^2} + \frac{1}{\delta y^2} \right) \right] \mathcal{P}_{i,j}^{n+1} = \frac{1}{2\delta t} \left(\frac{u_{i+1,j}^* - u_{i-1,j}^*}{\delta x} + \frac{v_{i,j+1}^* - v_{i,j-1}^*}{\delta y} \right) \quad (13)$$

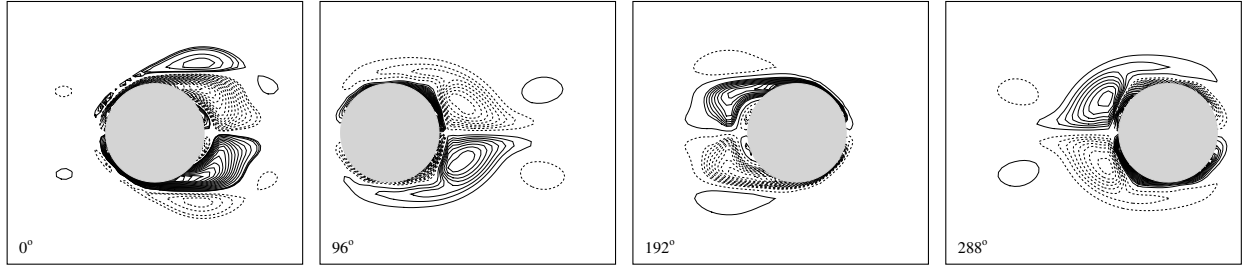


Figure 1: Vorticity isolines at four phases of oscillation. Dashed and solid lines indicate the negative and positive values, respectively.

3 Results and Conclusions

The oscillation of a circular cylinder in a quiescent fluid has been investigated frequently in the literature. This flow concerns two dimensionless parameters, i.e., the Reynolds number, $Re = U_{max}D/\nu$ and Keulegan-Carpenter number, $KC = U_{max}/fD$, where D is a characteristic length and f is the oscillation frequency. The motion of the cylinder is prescribed by $x_c(t) = -\frac{1}{2\pi} \sin(2\pi ft)$, where x_c indicates the location of the cylinder center. The Reynolds number and Keulegan-Carpenter numbers are set to 100 and 5, respectively. The computational domain is a square of size $20D$ in both directions with a circular cylinder initially located at the center of the domain. Vorticity isolines at four phase angles of oscillation after beginning the vortex shedding are shown in figure 1. The symmetric and anti-symmetric distribution of the u and v velocities along the y axis is shown in figure 2 which are in good agreement with the numerical data of [2] and [3].

The capability of the model to simulate the wave motion at the fluid interface under the effect of predetermined motion of a structure is also evaluated. The interface is captured for six phases of cylinder oscillation in figure 3. The frequency and amplitude of the oscillation are $\sqrt{g/R}$ and $1.75R$, where R is the cylinder radius. The initial vertical position of the cylinder is $0.3R$ underneath of the interface. Examples with a floating structure including comparison with benchmark results will be presented at the workshop.

REFERENCES

- [1] Amini-Afshar, M., Bingham, H. B., Henshaw, W. D., and Read, R. A nonlinear potential-flow model for wave-structure interaction using high-order finite differences on overlapping grids. In *Proceeding of the 34th International Workshop on Water Waves and Floating Bodies (IWWWF)* (2019).
- [2] Yang, J., and Balaras, E. 2006. *An embedded-boundary formulation for large-eddy simulation of turbulent flows interacting with moving boundaries*. *Journal of Computational Physics* 215(1), 12–40.
- [3] Dütsch, H., Durst, F., Becker, S., and Lienhart, H. 1998. *Low-Reynolds-number flow around an oscillating circular cylinder at low Keulegan–Carpenter numbers*. *Journal of Fluid Mechanics* 360, 249–271.
- [4] Raessi, M., and Pitsch, H. 2012. *Consistent mass and momentum transport for simulating incompressible interfacial flows with large density ratios using the level set method*. *Computers & Fluids* 63, 70–81.

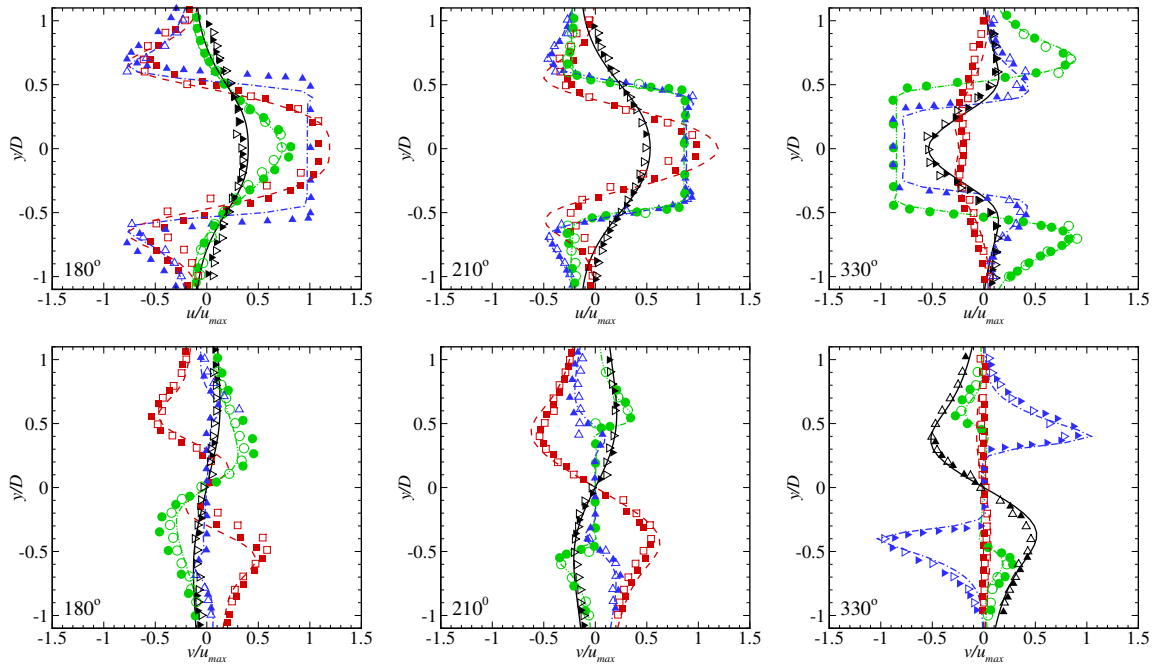


Figure 2: The velocity profiles u (top) and v (bottom) at four x locations in three phases of oscillation: $x = -0.6D$ ($- \square \blacksquare$), $x = 0.0D$ ($- \triangle \blacktriangle$), $x = 0.6D$ ($- \circ \bullet$) and $x = 1.2D$ ($- \triangleright \blacktriangleright$). The hollow and solid symbols correspond to the numerical and experimental data of [2] and [3], respectively, lines are the current calculations.

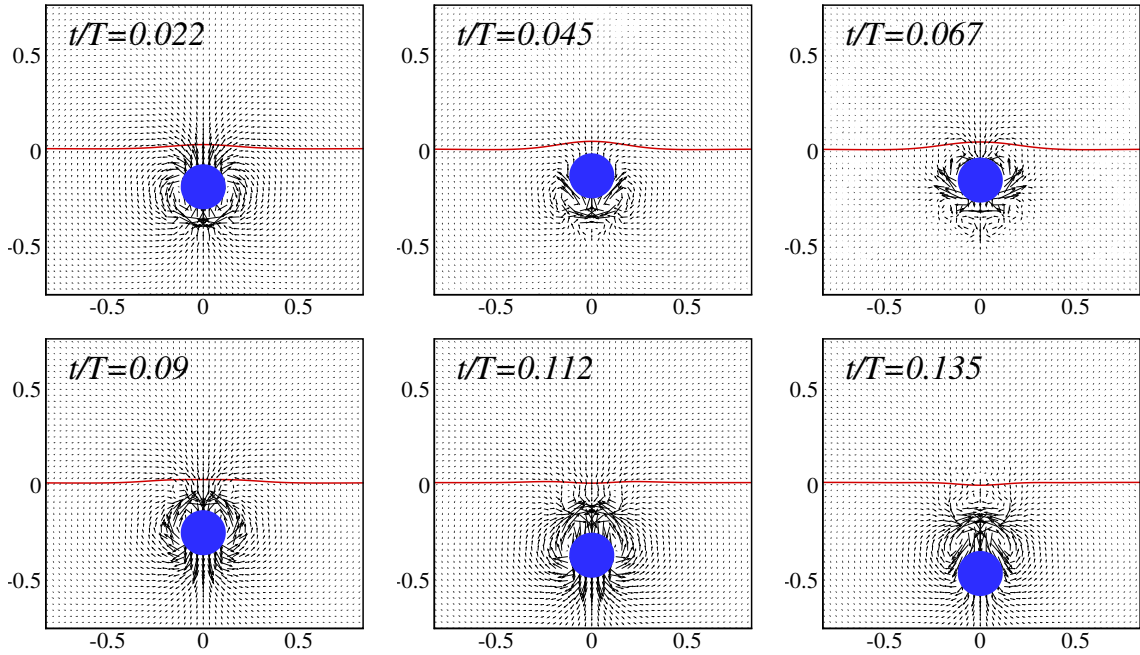


Figure 3: Waves generated by an oscillating submerged cylinder at various phases of the motion.